Received: 4 September 2018 | Revised: 28 October 2018 | Accepted: 29 October 2018

DOI: 10.1002/jmr.2772

RESEARCH ARTICLE

WILEY Journal of Molecular Recognition

Assembly of a miRNA-modified QCM sensor for miRNA recognition through response patterns

Xue Li[1] | Ding Ma[1] | Sheng-Run Zheng[1] | Jun Fan[1] | Tai Wang[2] | Zong Dai[3] | Xiao-Yong Zou[3] | Shao-Hua Teng[4] | Wei-Guang Zhang[1]

[1] School of Chemistry and Environment, South China Normal University, Guangzhou, China

[2] Research and Development Department, Guangzhou Research & Creativity Biotechnology Co. Ltd, Guangzhou, China

[3] School of Chemistry, Sun Yat-sen University, Guangzhou, China

[4] School of Computer Science and Technology, Guangdong University of Technology, Guangzhou, China

Correspondence
Sheng-Run Zheng and Wei-Guang Zhang, School of Chemistry and Environment, South China Normal University, Guangzhou 510006, China.
Email: zhengsr@scnu.edu.cn; wgzhang@scnu.edu.cn

Funding information
National Natural Science Foundation of China, Grant/Award Numbers: 21571070 and 21473062; Guangzhou Science and Technology Project, Grant/Award Numbers: 201604020145 and 201802010026; Guangdong Provincial Science and Technology Project, Grant/Award Number: 2016B010108007

Abstract

In this paper, a miRNA-based quartz crystal microbalance (QCM) biosensor was fabricated and used to the rapid and effective sensing of miRNA. The specific hybridization between probe miRNA and different selected miRNAs (miR-27a, miR-27b, and Let-7a) cause a different interaction mode, thus display different frequency change and response patterns in the QCM sensor, which were used to detect miR-27a and miR-27b. The selective sensing of miR-27a in mixed miRNA solution was also achieved. This miRNA-based QCM biosensor has the advantages of real-time, label-free, and short cycle detection.

KEYWORDS

miRNA, miR-27a, miR-27b, QCM sensor, response pattern

1 | INTRODUCTION

MiRNAs are an abundant class of short noncoding RNAs that are approximately 22 nucleotides in length.[1] They exist in most eukaryotic cells and play an important role in many biological processes, including cell proliferation, differentiation, and apoptosis, by inhibiting protein translation or accelerating messenger RNA (mRNA) degradation to regulate gene expression.[2-5] Recently, many researchers have shown that miRNA is closely related to many mortal diseases such as cancer and cardiovascular disease, and thus, miRNA has become a reliable marker of such diseases.[6-9] MiRNA-27a (miR-27a) as one of multifunctional miRNAs is expressed in various tissues, and the abnormal expression of miR-27a has been observed in various diseases such as colon cancer lymphangiogenesis, myocardial infarction, intervertebral disc degeneration, and so on,[10-15] while miRNA-27b (miR-27b) is related to gastric cancer, breast cancer, and so on.[16-18] Therefore, rapid and sensitive detection methods for such miRNAs are of great important in disease prevention, early detection, screening, diagnosis, and treatment.

Currently, probe hybridization and amplification technologies have been the most commonly used methods for miRNA quantification. Probe hybridization techniques include northern blotting,[19] in situ hybridization,[20] and microarrays[21] are well established but often require a large quantity of samples. Amplification technologies, including real-time fluorescent quantitative polymerase chain reaction (RT-PCR)[22] and rolling circle amplification (RCA),[23] are often time-consuming and complicated to operate. Recently, the quartz crystal microbalance (QCM) mass sensor has the characteristics of high sensitivity, label-free and, real-time analysis, and it has been widely used in biosensors.[20-25] Many studies have shown that DNA-modified QCM biosensors can be applied to detect such processes as DNA hybridization[26] and single base mismatch of DNA.[27] However, studies on QCM

biosensor for miRNA detection has been still limited.[28-30] There are only several examples. In 2016, Guo et al developed a miRNA-bound QCM sensor coupled with gold nanoparticle (GNP)/dendrimer-induced signal enhancement for recognition of miRNA-203, which good linear relationship between frequency change and the concentration of miRNA-203 was shown in the range of 1.0×10^{-11}–1.0×10^{-9} M.[29] In 2017, Premaratne et al[30] reported a QCM biosensor for the detection of miRNA-21, and the detection limit (LOD) was 28 fM when combined with a signal enhancement strategy. Therefore, the applications of the QCM sensor for miRNA detection is in its infancy. In this paper, a miRNA-modified QCM biosensor was fabricated and used for sensing miR-27a and miR-27b based on the miRNAs' interaction mode and frequency change.

2 | EXPERIMENTAL SECTION

2.1 | Materials and reagents

All the synthesized miRNA sequences were purchased from Sangon Biotech Co., Ltd. Their base sequences are showed in Table 1. 6-Mercapto-1-hexanol was purchased from the Platinia Love Shanghai Chemical Industry Development Co., Ltd (Shanghai, China). Phosphate-buffered saline (PBS; pH = 7.4) was purchased from Xiamen Haibiao Technology Co., Ltd (Xiamen, China). The other chemicals were of analytical reagent grade. Deionized water was used in all experiments. Concentrated sulfuric acid was purchased from the Zhuhai Huacheng Chemical Co., Ltd. Hydrogen peroxide (H_2O_2) was purchased from the Guangzhou Chemical Reagent Factory.

2.2 | Apparatus and measurements

All on-line detections were implemented on a homemade aqueous media measuring QCM system (Figure 1a). The system consisted of a QCM biosensor, a reaction cell, an oscillator detector, a frequency counter, and a computer. The AT-cut quartz crystals (13.0 mm diameter, 5 MHz resonant frequency) were covered with gold electrodes on both sides.

The miRNA quartz crystal sensors were prepared by using a two-step assembling process. First, the quartz gold piece was soaked in piranha solution (98% H_2SO_4:30% H_2O_2 (*v*/v) = 7:3) for 5–10 minutes, rinsed with deionized water, and dried with nitrogen. Second, the pretreated quartz gold piece was immersed in the mixture of 6-mercapto-1-hexanol (0.25mM) and probe miR-27a (from 0.1-1.5 μM) solution for 24 hours at a certain temperature (from −20°C-45°C) to form a miRNA-based biochip (Figure 1B).

TABLE 1 Sequences of miRNA used in this study

Name	Sequences(5′–3′)
Probe miRNA	HS-GCGGAACUUAGCCACUGUGAA
miR-27a	UUCACAGUGGCUAAGUUCCGC
miR-27b	UUCACAGUGGCUAAGUUCUGC
miR-let-7a	UGAGGUAGUAGGUUGUAUAGUU

All miRNA-sensing experiments were performed in a QCM cell. First, phosphate buffer was injected into the QCM cell, and the crystal frequency was measured as a background signal. After the signal change was less than 1 Hz of frequency drift in 5 minutes, the experiment could be continued. Then, the PBS solution with target miRNA in different concentrations was injected into the cell, and the solution in the QCM cell was kept still until a stable signal was obtained. Finally, another phosphate buffer was injected into the QCM cell again and the frequency was recorded.

3 | RESULTS AND DISCUSSION

3.1 | Self-assembly of miRNA-modified QCM biosensors

To obtain a miRNA-modified QCM biochip that has the strongest recognition ability with the target miRNA, the self-assembly of the miRNA-based QCM biochips was optimized. It has been reported that the surface coverage of probes immobilized on gold surfaces is important,[31] and thus, 6-mercapto-1-hexanol was used to regulate the surface coverage of the probe miR-27a. Considering that the temperature and ratio of 6-mercapto-1-hexanol and probe miR-27a may be the most important factors that determine the self-assembly processes, the influences of the temperature and concentration ratio were investigated. Because the hybridization between the probe miRNA and complementary miR-27a would enhance the mass on the surface of QCM sensor and reduce the frequency, thus frequency variation Δf of the miRNA-modified QCM biochips when interacting with miR-27a was used as an evaluation index.

As shown in Table S1 and Figure 2A. The Δf value first increased and then decreased with the increase of temperature in the range from −20°C to 45°C, and it reaches a maximum value at 5°C. The influence of temperature is complicated. It can affect the thermodynamics and kinetics of the formation of Au-S bonds between 6-mercapto-1-hexanol/miRNA and gold surface, thus affecting the competitive reaction between 6-mercapto-1-hexanol and miRNA. Since the formation of Au-S is an exothermic reaction, it is clear that lower temperature may be favorable for assembly, but lower temperature will also lead to lower reaction rate and may reduce the coverage of miRNA. Therefore, the best temperature obtained by the experiment is approximately at an intermediate temperature of −20°C to 45°C, which is 5°C.

The influence of the probe miRNA concentration is given in Table S2 and Figure 2B. With the increase of the concentration from 0.1 μM to 1.5 μM, the ▵f gradually increased, reached the highest value at 1.0 μM, and then gradually decreased. Therefore, 1.0 μM was determined as the optimal concentration of the probe miR-27a for the QCM. The coverage of the miRNA on QCM biochip is influenced by the concentration of the probe miRNA and the competitive reagents. The lower probe miRNA concentration gives lower coverage, thus fewer target miRNAs would be hybridized and the ▵f would be smaller. As the concentration increases, the ▵f increase to reach the highest value. After that, the increases of the coverage may result in smaller space between probe miRNAs, which is not conducive to the

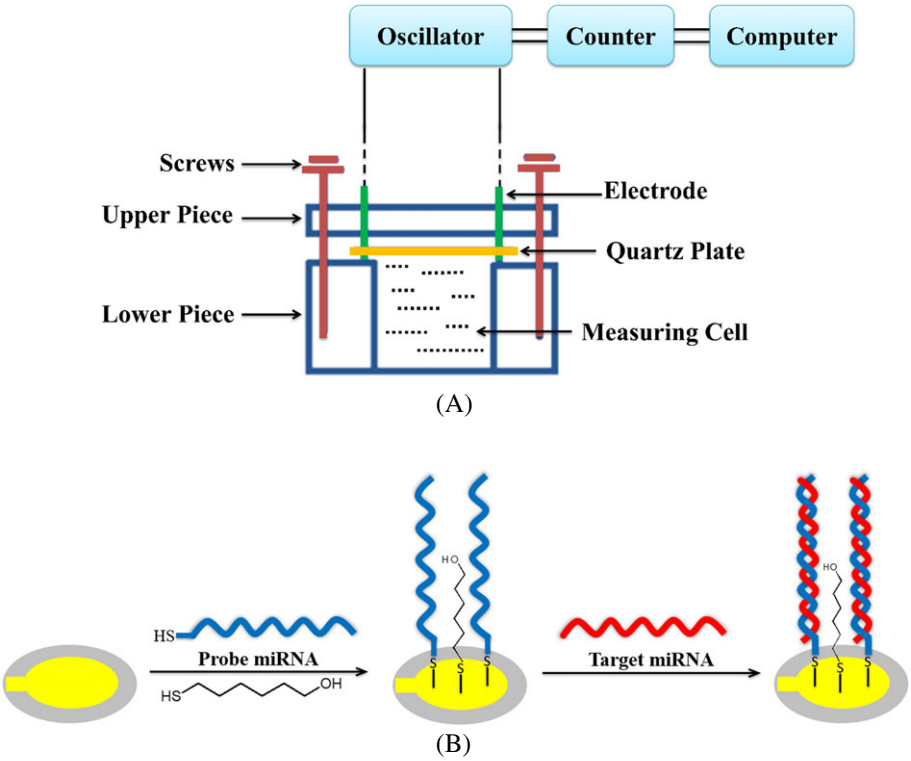

FIGURE 1 A, Schematic diagram of static detection quartz crystal microbalance sensor system. B, Self-assembly and detection process of the QCM-microRNA sensor

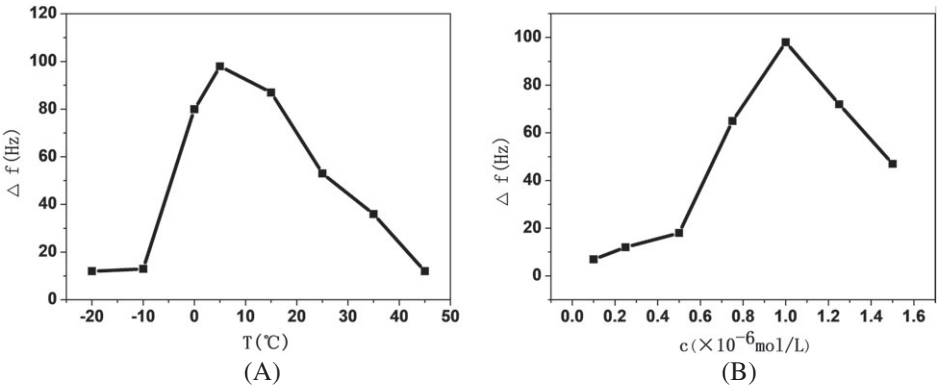

FIGURE 2 A, Effect of temperatures and B, effect of probe miR-27a concentrations on the assembly of microRNA-modified sensor

hybridization of the target miRNA, thus the frequency change is reduced.

3.2 | Interaction patterns between probe miR-27a and three miRNAs

Three miRNAs, miR-27a that is complementary to the probe miRNA, miR-27b that has a single base mismatch to the probe miRNA, and miR-let-7a that is completely mismatched to the probe miRNA, were selected to study the sensing ability of miRNA-modified biosensor toward different miRNAs. As shown in Figure 3, after the miR-27a solution (0.5×10^{-6} M) was injected into the QCM sensor, the frequency of the sensor was significantly decreased and remained almost unchanged at about 5000 seconds, in which the maximum change of frequency was about −127 Hz. After that, the PBS buffer was injected at 5000 seconds, and the frequency was not obviously changed, with only another 3 Hz reduction at 10 000 seconds. Then, the PBS buffer solution (0.20 mL) was injected and the frequency kept stable. Then, another miR-27a solution and another PBS buffer was alternatively injected again several times but did not bring a significant frequency change. These results indicate that the hybridization of probe miRNA and complementary miR-27a was effective and easy to be detected by QCM, the frequency change is comparable with those reported QCM sensors.[29,30]

For single-base mismatch miR-27b, the frequency was decreased gradually and the frequency change reached to −24 Hz after 5000 seconds when the PBS buffer of 0.5×10^{-6} M miR-27b was injected into

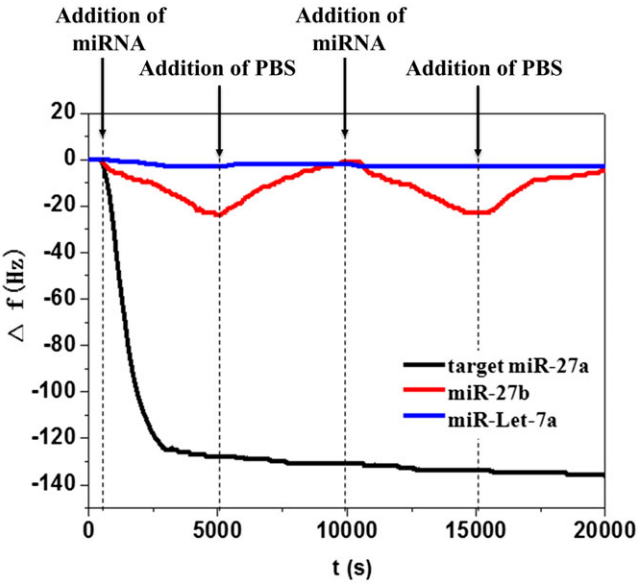

FIGURE 3 Frequency change patterns of the quartz crystal microbalance (QCM) sensor with miR-27a, miR-27b, and miR-let-7a

the QCM sensor. Then, the PBS buffer was injected and the frequency was increased gradually, reaching −1 Hz at 10 000 seconds. Such a frequency change pattern can be repeated by injecting miR-27b and PBS solution again at 10 000 and 15 000 seconds, respectively. These results indicate that the hybridization of probe miR-27a and miR-27b was relatively ineffective, and thus, the probe miR-27a/miR-27b composite can be converted back to single-strand miRNA when eluted by PBS solution.

When injecting miR-let-7a, the frequency of the QCM sensor did not change, indicating the lack of interaction between the probe miR-27a and miR-let-7.

As described above, the frequency change patterns of the three miRNAs are totally different, which can be attributed to the different interactions between the probe miR-27a and the three miRNAs. Both miR-27a and miR-27b can reduce the frequency of QCM sensors via their interactions with the probe miRNA. Therefore, it is not reliable to detect them only by the frequency change.[27] However, if the frequency change pattern (reduced gradually and reduced and increased repeatedly for miR-27a and miR-27b, respectively) is considered at the same time, it is more reliable to distinguish them.

3.3 | Analysis of miRNA

The frequency changes upon the addition of miR-27a and miR-27b at different concentrations were measured. As shown in Figure 4A, the frequency changes significantly decreased from −11 to −127 Hz along with increasing the concentration of miR-27a from 0.2×10^{-6} to 0.45×10^{-6} M. The frequency change (Hz) versus the miR-27a concentration (10^{-6} M) follows a simple exponential equation y = −46.25315 + 24.27145exp (3.94193x) obtained by the least-squares fitting method with a correlation coefficient (R^2) of 0.97422 (Figure 4b).

As shown in Figure 5a, the frequency changes significantly decreased from −1 to −24 Hz through increasing the concentration of miR-27b from 0.2×10^{-6} M to 0.45×10^{-6} M, indicating that the sensitivity is significantly lower than that of miR-27a. The frequency change versus the miR-27b concentration (10^{-6} M) follows a simple linear equation y = −17.10714 + 80.71429x obtained by the least-squares fitting method with a correlation coefficient (R^2) of 0.97723 (Figure 5B).

For comparison, the frequency changes upon addition of miR-let-7a at different concentrations were also measured. The frequency did not obviously change as expected. All of the data are summarized in Table S3.

3.4 | Selectivity

To examine the selectivity of this sensor to detect specific miRNA, we conducted a study on mixed miRNA targets. As shown in Figure 6, the mixture of single-base mismatch miR-27b and miR-Let-7a (both are 0.5×10^{-6} mol/L) and the mixture of complementary miR-27a and miR-let-7a (both are 0.5×10^{-6} mol/L) gave frequency changes of −29 Hz and − 135 Hz, respectively. These changes are close to those of the single miR-27a (−127 Hz) and miR-27b (−24 Hz), respectively. Therefore, the mismatch miR-Let-7a had no significant influence on the frequency change. Interestingly, the mixed complementary miR-

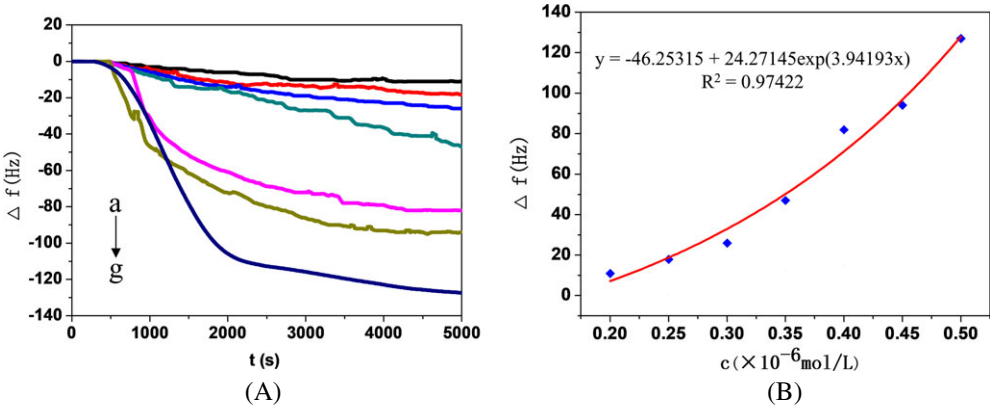

FIGURE 4 A, Real-time frequency responses of the miRNA-modified quartz crystal microbalance (QCM) sensor with addition miR-27a. From a to g: 0, 0.2, 0.25, 0.3, 0.35, 0.4, 0.45, and 0.5 μM miR-27a in PBS solution. B, The initial miR-27a concentration was correlated with the frequency change through an exponential relationship

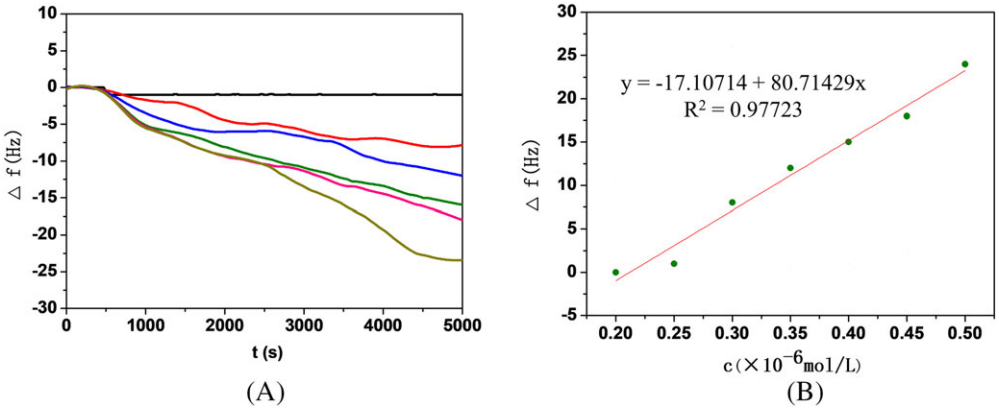

FIGURE 5 A, Real-time frequency responses of the miRNA-modified quartz crystal microbalance (QCM) sensor for miR-27b detection. From a to g: 0, 0.2, 0.25, 0.3, 0.35, 0.4, 0.45, and 0.5 μM miR-27b in phosphate-buffered saline (PBS) solution. B, The initial miR-27b concentration was correlated with the frequency change by a linear relationship

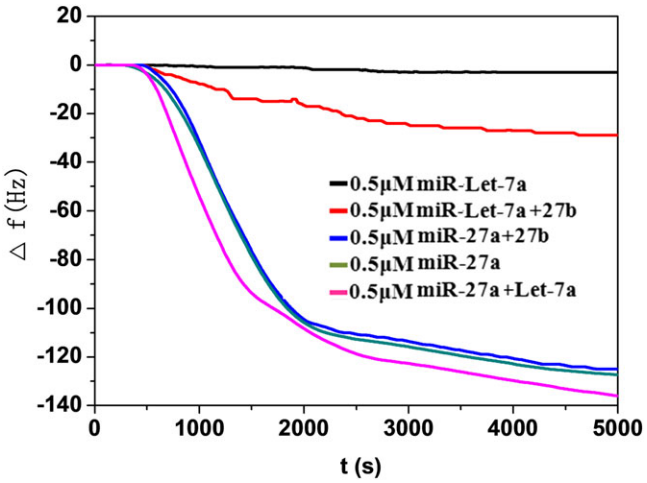

FIGURE 6 Real-time frequency responses of the miRNA-modified quartz crystal microbalance (QCM) sensor for the detection of different mixed miR-RNAs

27a and single-base mismatch miR-27b (both are 0.5 × 10^{-6} mol/L) gave a frequency change of −124 Hz, which is also close to that of only miR-27a (127 Hz). This indicates that the perfectly matched RNA–RNA hybrid is preceded by nonperfect RNA–RNA hybrid with a nucleotide mismatch, which were often observed,[25,32,33] and thus, the frequency changes triggered by the single-base mismatched target were very small when competing with the complementary target. These results indicate that the sensor has potential to detect biological samples.

4 | CONCLUSIONS

In conclusions, a miRNA-modified QCM sensor for the qualitative or quantitative detection of miRNA is prepared. The specific interactions caused by hybridization between the probe miR-27a and target miRNA (completely complementary, single-base mismatch, and complete mismatch miRNA) are discussed. Qualitative detection of complementary and single base mismatch miRNA can be achieved based on their interaction patterns. In addition, quantified detection can also be achieved by detecting the frequency change, in which the minimum detection concentration of the target miR-27a is 0.2 × 10^{-6} mol/L without any enhancement strategy.

ACKNOWLEDGEMENTS

This work was financially supported by the National Natural Science Foundation of China (grant no. 21571070 and 21473062), the Guangdong Provincial Science and Technology Project (No.2016B010108007), and the Guangzhou Science and Technology Project (No 201802010026 and 201604020145).

CONFLICTS OF INTEREST

There are no conflicts to declare.

AUTHOR CONTRIBUTIONS

All authors have read and approved the final manuscript. X. Li and D. Ma performed the research. Z. Dai, X.-Y. Zou, S.-H. Teng and W.-G. Zhang designed the research study. S.-R. Zheng, J. Fan and T. Wang wrote the paper.

ORCID

Sheng-Run Zheng https://orcid.org/0000-0002-9071-0748
Wei-Guang Zhang http://orcid.org/0000-0002-3697-2990

REFERENCES

1. Graybill RM, Bailey RC. Emerging biosensing approaches for microRNA analysis. *Anal Chem*. 1994;88(1):431-450.
2. Cortez MA, Calin GA. MicroRNA identification in plasma and serum: a new tool to diagnose and monitor diseases. *Expert Opin Biol Ther*. 2009;9(6):703-711.
3. Bartel DP. MicroRNAs: genomics, biogenesis, mechanism, and function. *Cell*. 2004;116(2):281-297.
4. Croce CM. Causes and consequences of microRNA dysregulation in cancer. *Nat Rev Genet*. 2009;10(10):704-714.
5. Teague EM, Print CG, Hull ML. The role of microRNAs in endometriosis and associated reproductive conditions. *Hum Reprod Update*. 2010;16(2):142-165.
6. Boeri M, Verri C, Conte D, et al. MicroRNA signatures in tissues and plasma predict development and prognosis of computed tomography detected lung cancer. *Proc Natl Acad Sci U S A*. 2011;108(9):3713-3718.

7. Liu G, Friggeri A, Yang Y, et al. MiR-21 mediates fibrogenic activation of pulmonary fibroblasts and lung fibrosis. *J Exp Med*. 2010;207(8):1589-1597.
8. Pottelberge GRV, Mestdagh P, Bracke KR, et al. MicroRNA expression in induced sputum of smokers and patients with chronic obstructive pulmonary disease. *Am J Respir Crit*. 2011;183(7):898-906.
9. Hu Z, Chen X, Zhao Y, et al. Serum MicroRNA signatures identified in a genome-wide serum microRNA expression profiling predict survival of non-small-cell lung cancer. *J Clin Oncol*. 2010;28(10):1721-1726.
10. Ji J, Zhang J, Huang G, Qian J, Wang X, Mei S. Over-expressed microRNA-27a and 27b influence fat accumulation and cell proliferation during rat hepatic stellate cell activation. *FEBS Lett*. 2009;583(4):759-766.
11. Liu T, Tang H, Lang Y, Liu M, Li X. MicroRNA-27a functions as an oncogene in gastric adenocarcinoma by targeting prohibitin. *Cancer Lett*. 2009;273(2):233-242.
12. Ma Y, Yu S, Zhao W, Lu Z, Chen J. MiR-27a regulates the growth, colony formation and migration of pancreatic cancer cells by targeting Sprouty2. *Cancer Lett*. 2010;298(2):150-158.
13. Cai M, Cheng J, Zhou M, et al. The association between pre-miR-27a rs895819 polymorphism and myocardial infarction risk in a Chinese Han population. *Lipids Health Dis*. 2018;17(1):7.
14. Wang Q, Li DC, Li ZF, et al. Upregulation of miR-27a contributes to the malignant transformation of human bronchial epithelial cells induced by SV40 small T antigen. *Oncogene*. 2011;30(36):3875-3886.
15. Xu LL, Xiang JY, Shen J, et al. Oncogenic microRNA-27a is a target for genistein in ovarian cancer cells. *Anticancer Agents Med Chem*. 2013;13(7):1126-1132.
16. Feng QZ, Wu XL, Li FC, et al. miR-27b inhibits gastric cancer metastasis by targeting NR_2F_2. *Protein Cell*. 2017;8(2):114-122.
17. Miao X, Rahman MFU, Jiang L, et al. Thrombin-reduced miR-27b attenuates platelet angiogenic activities in vitro via enhancing platelet synthesis of anti-angiogenic thrombospondin-1. *J Thromb Haemost*. 2018;16(4):791-801.
18. Chen XJ, Cui YJ, Xie XH, Xing YF, Yuan XH, Wei YM. Functional role of miR-27b in the development of gastric cancer. *Mol Med Rep*. 2018;17(4):5081-5087.
19. Anna V, Hornyik C, Varga N, Burgyan J, Kauppinen S, Havelda Z. Sensitive and specific detection of microRNAs by northern blot analysis using LNA-modified oligonucleotide probes. *Nucleic Acids Res*. 2004;32(22):e175.
20. Kloosterman WP, Wienholds E, Brujin ED, Kauppinen S, Plasterk RHA. In situ detection of miRNAs in animal embryos using LNA-modified oligonucleotide probs. *Nat Methods*. 2006;3(1):27-29.
21. Song W, Guo X, Sun W, et al. Target-triggering multiple-cycle signal amplification strategy for ultrasensitive detection of DNA based on QCM and SPR. *Anal Biochem*. 2018;553:57-61.
22. Dultsev FN, Kolosovsky EA, Lomzov AA, Pyshnyi DV. QCM-based rupture force measurement as a tool to study DNA dehybridization and duplex stability. *Anal Bioanal Chem*. 2017;409(4):891-901.
23. Bunroddith K, Viseshakul N, Chansiri K, Lieberzeit P. QCM-based rapid detection of PCR amplification products of Ehrlichia Canis. *Anal Chim Acta*. 2018;1001:106e111.
24. Yao C, Zhu T, Tang J, et al. Hybridization assay of hepatitis B virus by QCM peptide nucleic acid biosensor. *Biosens Bioelectron*. 2008;23(6):879-885.
25. Li H, Xiao S, Yao D, Lam MHW, Liang H. A smart DNA–gold nanoparticle probe for detecting single-base changes on the platform of a quartz crystal microbalance. *Chem Commun*. 2015;51(22):4670-4673.
26. Liu CG, Calin GA, Meloon B, et al. An oligonucleotide microchip for genome-wide microRNA profiling in human and mouse tissues. *PNAS*. 2004;101(26):9740-9744.
27. Chen CF, Ridzon DA, Broomer AJ, et al. Real-time quantification of microRNAs by stem–loop RT–PCR. *Nucleic Acids Res*. 2005;33(20):e179.
28. Cheng YQ, Zhang X, Li ZP, Jiao XX, Wang YC, Zhang YL. Highly sensitive determination of microRNA using target-primed and branched rolling-circle amplification. *Angew Chem Int Ed*. 2009;48(18):3268-3272.
29. Guo YS, Wang YJ, Yang GX, Xu JJ, Chen HY. MicroRNA-mediated signal amplification coupled with GNP/dendrimers on a mass-sensitive biosensor and its applications in intracellular rmicroRNA quantification. *Biosens Bioelectron*. 2016;85:897-902.
30. Premaratne G, Mubarak ZHA, Senavirathna L, Liu L, Krishnan S. Measuring ultra-low levels of nucleotide biomarkers using quartz crystal microbalance and SPR microarray imaging methods: a comparative analysis. *Sensor Actuat B-Chem*. 2017;253:368-375.
31. Herne TM, Tarlov MJ. Characterization of DNA probes immobilized on gold surfaces. *J Am Chem Soc*. 1997;119(38):8916-8920.
32. Rasheed PA, Sandhyarani N. Quartz crystal microbalance genosensor for sequence specific detection of attomolar DNA targets. *Anal Chim Acta*. 2016;905(28):134-139.
33. Patolsky F, Lichtenstein A, Willner I. Electronic transduction of DNA sensing processes on surfaces: amplification of DNA detection and analysis of single-base mismatches by tagged liposomes. *J Am Chem Soc*. 2001;123(22):5194-5205.

SUPPORTING INFORMATION

Additional supporting information may be found online in the Supporting Information section at the end of the article.

How to cite this article: Li X, Ma D, Zheng S-R, et al. Assembly of a miRNA-modified QCM sensor for miRNA recognition through response patterns. *J Mol Recognit*. 2018;e2772. https://doi.org/10.1002/jmr.2772